

# PHYSICAL REVIEW E

## STATISTICAL PHYSICS, PLASMAS, FLUIDS, AND RELATED INTERDISCIPLINARY TOPICS

---

THIRD SERIES, VOLUME 53, NUMBER 6 PART B

JUNE 1996

---

### ARTICLES

---

#### Coarsening dynamics of field-induced inversion domain walls in smectic-*C* films

Bongsoo Kim,<sup>1</sup> Sung Jong Lee,<sup>2</sup> and Jong-Rim Lee<sup>3</sup>

<sup>1</sup>*Department of Physics, Changwon National University, Changwon 641-773, Korea*

<sup>2</sup>*Department of Physics, The University of Suwon, Suwon 445-743, Korea*

<sup>3</sup>*Department of Physics, Pusan National University, Pusan 609-735, Korea*

(Received 9 November 1995)

We present a numerical study on the phase-ordering kinetics of the smectic-*C* film under an external magnetic field. Due to the inversion symmetry of the director fields, the external field induces Ising-like inversion domain walls in this system. It is observed that the usual dynamic scaling based on a single dominant length scale is violated for the Ising-like order parameter, except in the asymptotic time limit. This scaling violation is attributed to the existence of point defects along the domain walls and the corresponding length scale (the average separation between point defects) in addition to the average domain size. The correlation functions exhibit a very slow approach to the asymptotic scaling limit, with early-time correlation functions characterized by large curvature near the origin, gradually crossing over to Ising-like correlation functions at the late-time stage. In spite of this apparent violation of dynamic scaling, we find that the above slow approach toward the asymptotic pure Ising scaling function follows a universal functional form when the time is properly rescaled in terms of the field-dependent time scale. [S1063-651X(96)11705-7]

PACS number(s): 64.70.Md, 64.60.Cn, 64.60.My, 82.20.Mj

#### I. INTRODUCTION

Understanding the ordering kinetics of statistical systems that are subjected to a rapid thermal quench from a disordered phase to an ordered phase has long been one of the central issues in nonequilibrium statistical mechanics [1–3]. Recent nonperturbative approaches [4–6] to this problem seem to provide significant theoretical progress in this area. By being extended to systems possessing continuous degeneracy of ground states, the theory [7–9] has stimulated intensive theoretical and experimental investigations on the kinetics of systems having a variety of stable topological defects such as vortices, strings, and monopoles. In spite of this important progress, it appears that the effects of symmetry-breaking external fields on the phase-ordering kinetics have been less well studied [10,11].

It is noteworthy that liquid crystal systems [12] have served as an appropriate test ground for important theoretical predictions made for phase-ordering kinetics of systems possessing continuous symmetry [13]. At the same time, for these systems many equilibrium studies on the effects of external fields have been carried out. Helfrich [14], de Gennes [15], Brochard [16], and others [17] have studied equilibrium profiles of inversion domain walls induced by an

external magnetic field subjected to various anchoring conditions of the glass plates between which liquid crystal samples are placed. Pindak *et al.* [18] have observed a macroscopic pattern of  $2\pi$ -disclination walls in a ferroelectric smectic-*C* film under external electric fields.

One can imagine a nonequilibrium situation where a smectic-*C* film is quenched from an isotropic disordered phase under external magnetic fields. In this situation, the field-induced inversion domains will coarsen as the system evolves toward its equilibrium ordered phase. In the present work, we report a numerical investigation of growth kinetics of these inversion domains. A similar numerical simulation has been carried out by Pargellis *et al.* [19] with the motivation quite different from that of the present study: their experimental observation on the coarsening process of a free standing smectic film (with no external field) did not agree with the theoretical expectation based on the two-dimensional *XY* model. For example, while in the two-dimensional *XY* model the defect density shows a power-law decay, the experimental result exhibited an exponential decay for the same quantity. In order to resolve this discrepancy, they invoked an internal field and its dipole coupling to the director field. Focusing on this issue, they did not deal with the detailed aspects of the growth and coarsening of the inversion domains.

We summarize briefly in the following the main results of the present work. First, we find that the usual dynamic scaling based on a single dominant length scale is systematically violated in the equal-time correlation functions for the Ising-like order parameter, except in the asymptotic time limit. This scaling violation may be attributed to the existence of another length scale (in addition to the average domain size) corresponding to the average separation between point defects residing on the domain walls. The average size of domains  $L_I(t)$  begins, at the early stage of ordering, as  $L_I(t) \sim t^{\phi_1}$  with  $\phi_1 \approx 0.38$ , and then crosses over at the late-time stage to  $\phi_2 \approx 0.46$ , which is close to the curvature-driven growth exponent  $1/2$ .

It is possible to identify a time scale  $\tau(h)$  depending on the magnetic field  $h$ , with which we can rescale the time dependence of the domain size for various values of  $h$ . When  $L_I(t)$  is measured in units of  $\xi$ , the equilibrium width of domain walls, this procedure results in a fairly good collapse of the time dependence of the domain size for different values of the external field. The same time scale  $\tau(h)$  can be used to rescale the time dependence of the excess energy relaxation and also in rescaling the systematic approach to the asymptotic (Ising) limit for the equal time correlation functions.

This paper is organized as follows. In Sec. II, the model and the simulation methods are described. The main results of our simulations are presented in Sec. III along with the discussions on the results, which is followed by Sec. IV, summarizing the main features of this work.

## II. THE MODEL

The elastic free energy for smectic- $C$  film under a magnetic field [12], assuming the equal elastic constants, is given by

$$F[n] = \int d^2r \left[ \frac{K}{2} (\vec{\nabla} \vec{n})^2 + \frac{g}{4} (\vec{n}^2 - 1)^2 - \frac{\chi}{2} (\vec{n} \cdot \vec{h})^2 \right], \quad (1)$$

where the first term represents the elastic energy cost for distortion of the director field  $\vec{n}$ , the second one drives the director field into unit length in the absence of the external field, and the last denotes the coupling of the director field to the external uniform magnetic field. The parameters  $K$ ,  $g$ , and  $\chi$  denote the isotropic elastic constant, the rigidity of the director, and the magnetic susceptibility, respectively. In the present case, the director field  $\vec{n}$  is a two-component real vector field, which characterizes the in-plane molecular orientation in smectic- $C$  film. The dynamic equation governing the evolution of the system toward equilibrium is assumed to be the model A [20], appropriate to systems with nonconserved order parameters, of the form

$$\frac{\partial \vec{n}}{\partial t} = - \frac{\delta F}{\delta \vec{n}} = K \nabla^2 \vec{n} + g(1 - \vec{n}^2) \vec{n} + \chi (\vec{n} \cdot \vec{h}) \vec{h}, \quad (2)$$

where the thermal noise is ignored since we consider the case of zero-temperature quench only.

Due to the presence of the symmetry-breaking external field, the  $O(2)$  symmetry is broken and the inversion symmetry of the director field generates the discrete Ising-like

double degeneracy of the ground states. Therefore, defining an Ising-like order parameter  $\sigma = \vec{n} \cdot \hat{h}$  where  $\hat{h}$  is the unit vector along the direction of the external magnetic field, one can obtain dynamic equation for the order parameter field  $\sigma$ . In order to do so, it is convenient to decompose the director field  $\vec{n}$  into components along the directions  $\hat{h}$  and  $\hat{t}$  parallel and normal to the magnetic field, respectively:

$$\vec{n}(\vec{r}, t) = \sigma(\vec{r}, t) \hat{h} + \pi(\vec{r}, t) \hat{t}. \quad (3)$$

Multiplying (2) with the unit vectors  $\hat{h}$ ,  $\hat{t}$  respectively, we obtain the following set of dynamic equations for the two fields  $\sigma$  and  $\pi$ :

$$\frac{\partial \sigma}{\partial t} = K \nabla^2 \sigma + g \left( 1 + \frac{\chi h^2}{g} - \sigma^2 - \pi^2 \right) \sigma, \quad (4)$$

$$\frac{\partial \pi}{\partial t} = K \nabla^2 \pi + g(1 - \sigma^2 - \pi^2) \pi. \quad (5)$$

From Eqs. (4) and (5) we can obtain the ground-state configurations  $\sigma = \pm \sqrt{1 + h^2}$  and  $\pi = 0$  with the ground-state energy  $E_G = -h^2(h^2 + 2)/4$ . The equilibrium profile of an isolated straight domain wall (infinitely extended) is obtained by solving the set of stationary equations resulting from (4) and (5),

$$K \frac{d^2 \sigma}{dy^2} = -g \left( 1 + \frac{\chi h^2}{g} - \sigma^2 - \pi^2 \right) \sigma, \quad (6)$$

$$K \frac{d^2 \pi}{dy^2} = -g(1 - \sigma^2 - \pi^2) \pi, \quad (7)$$

where  $y$  is the coordinate normal to the wall.

In the hard spin limit, i.e.,  $g \rightarrow \infty$ , one can represent the two fields  $\sigma$  and  $\pi$  in terms of a phase angle  $\theta$  with respect to the direction of magnetic field  $\hat{h}$  as one does in the  $XY$  model:  $\sigma = \cos \theta$ ,  $\pi = \sin \theta$ . Using this representation, one can obtain from (6) and (7) the equation for the phase angle  $\theta$  of the form

$$K \frac{d^2 \theta}{dy^2} = \frac{\chi h^2}{2} \sin(2\theta). \quad (8)$$

This is a sine-Gordon equation whose solution is given by  $\theta(y) = 2 \tan^{-1}[\exp(y/\xi)]$ , provided  $\theta(y=0) = \pi/2$ , where  $\xi = \sqrt{K/\chi h^2}$  is the equilibrium width of the domain wall. Note that it is inversely proportional to the strength of the magnetic field.

Simulation is carried out by directly integrating in time Eq. (2) with random initial conditions using the Euler algorithm with the integration time step  $\Delta t = 0.1$  on a square lattice with linear size  $N = 400$ . The integration is performed up to  $t = 1280$ . The Laplacian in (2) is discretized with the mesh size  $\Delta x = \Delta y = 1$ . Periodic boundary conditions in both lattice directions are employed. The parameters  $K$ ,  $g$ , and  $\chi$  are all set equal to unity and the direction of the uniform magnetic field is taken to be along the  $x$  axis:  $\vec{h} = h \hat{x}$ .

In order to probe the growth of the inversion domain walls, we compute the equal-time correlation function  $C(\vec{r}, t) = \langle \sigma(\vec{0}, t) \sigma(\vec{r}, t) \rangle$  for the Ising-like order parameter  $\sigma$ , the excess energy relaxation, and the time dependence of the number of point defects, where  $\langle \rangle$  denotes the average over random initial configurations. Here the average was taken over 30 to 60 different random initial configurations. It should be emphasized that the random initial conditions are not biased by the external magnetic field.

### III. SIMULATION RESULTS AND DISCUSSIONS

Before presenting the details of the simulation results, we briefly summarize the characteristic features of the pure Ising domain growth for the case of the nonconserved order parameter [1–3]. An important feature associated with the Ising growth is its self-similar nature, which is reflected in a scaling collapse of the equal-time correlation functions for the Ising order parameter computed at different times with the appropriate length scale  $L(t)$ , i.e.,  $C(\vec{r}, t) = f[r/L(t)]$ ,  $f(x)$  being the scaling function resulting from the collapse of the correlation functions. This dynamic scaling implies that there is a dominant *single* length scale in the ordering process that is regarded as the average size of Ising domains. The characteristic time dependence of the length scale  $L(t)$ , the growth law, is known to be  $L(t) \sim t^{1/2}$ , coming from the fact that the motion of domain wall is driven purely by its local curvature.

Equivalently, the dynamic structure factor  $S(\vec{k}, t)$ , the Fourier transform of  $C(\vec{r}, t)$ , has the corresponding scaling form

$$S(\vec{k}, t) = \int d^d r e^{i\vec{k} \cdot \vec{r}} C(\vec{r}, t) = L^d(t) g(kL(t)), \quad (9)$$

where  $g(y)$  is the Fourier transform of the scaling function  $f(x)$ . The short distance part of the scaling function  $f(x)$  is of the form

$$f(x) = 1 - \text{const} \times x, \quad x \ll 1. \quad (10)$$

This short distance behavior, known as Porod's law [21], is a direct consequence of sharpness of the domain walls (the thickness of the wall is very small compared to the average domain size). This behavior is also manifested in the scaling function of the dynamic structure factor as a power-law tail in the large wave-vector limit, i.e.,

$$g(y) \sim y^{-(d+1)}, \quad y \gg 1, \quad (11)$$

which becomes  $g(y) \sim y^{-3}$  for  $d=2$ . The excess energy shows a power-law decay of the form

$$\Delta E(t) \sim L(t)^{-1} \sim t^{-1/2}. \quad (12)$$

This behavior comes from the fact that the energy is dissipated mostly near the domain walls.

We now turn to discuss our simulation results. In order to see if the growth of the inversion domains exhibits self-similar morphology, we introduce an appropriate length scale  $L_I(t)$  defined as  $C[r=L_I(t), t] = 1/2$  for a given time  $t$ . Then the order-parameter correlation functions are plotted

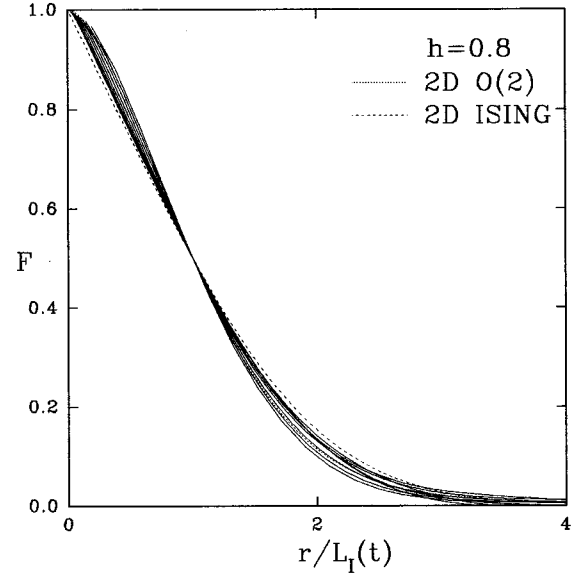


FIG. 1. Scaled correlation functions  $C[r/L_I(t), t]$  at different times  $t=10, 20, 40, 80, 160, 320, 640, 1280$  for  $h=0.8$ , where the length scale  $L_I(t)$  is defined as  $C[r=L_I(t), t]=1/2$ . The simple dynamic scaling is clearly violated.

against the scaled distance  $r/L_I(t)$ . If these plots are collapsed onto a single master curve, then the equal-time correlation function satisfies a dynamic scaling  $C(r, t) = f[r/L_I(t)]$ ,  $f(x)$  being the scaling function independent of time. However, for the present case, as Fig. 1 clearly shows, this procedure does not lead to a single curve onto which all correlation functions collapse. In order to see this scaling violation more closely, we focus in Fig. 2 on the short-distance part of the scaled correlation functions and for comparison we also show the scaling functions for the pure

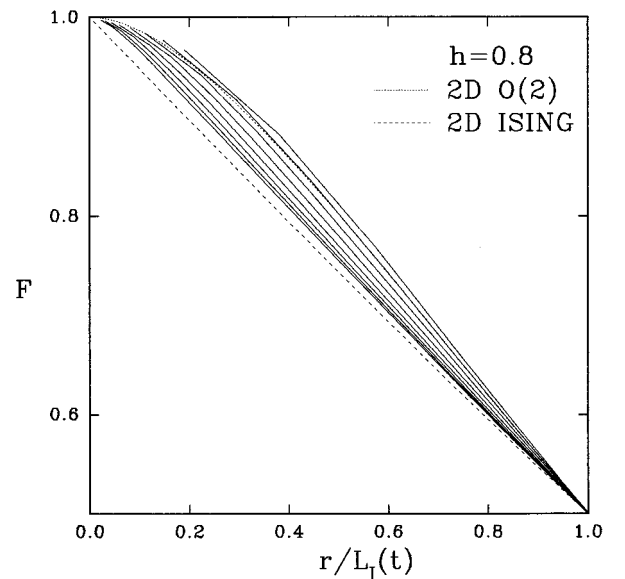


FIG. 2. Short-distance part of the scaled correlation functions in Fig. 1, which shows a slow approach of the scaled correlation function to the pure Ising correlation function. Note that it has a considerable curvature at early time stages.

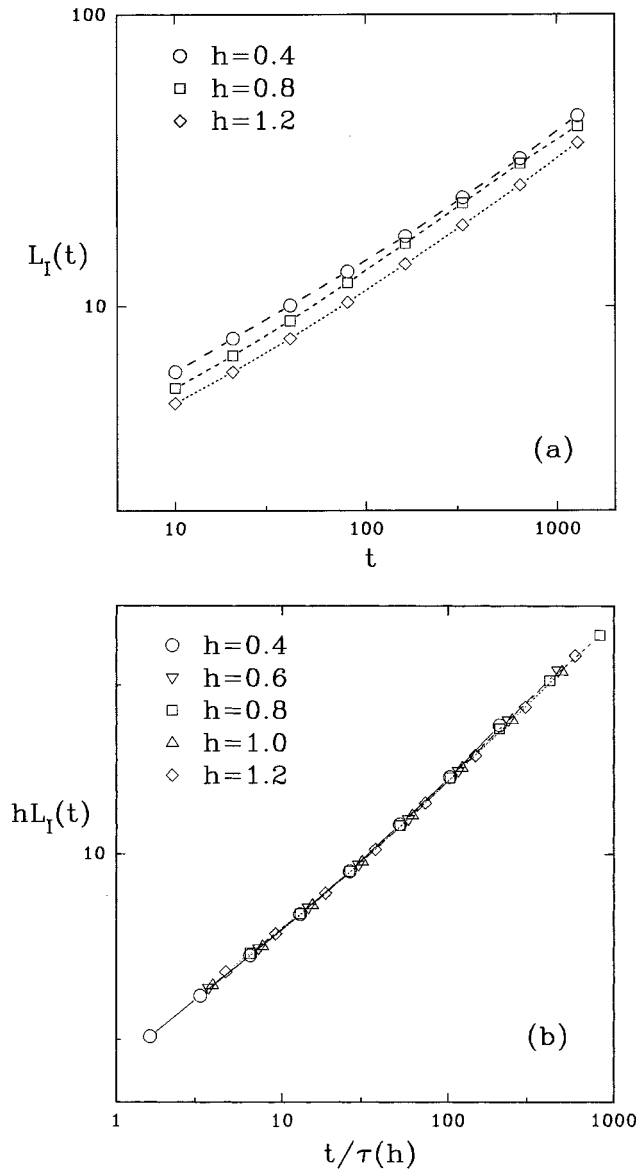


FIG. 3. (a) Time dependence of the length scale  $L_I(t)$  for several external fields. (b) Scaling of the length scales  $L_I(t)$  using the field-dependent time scale  $\tau(h)$ .

$O(2)$  model and the Ising model both in two dimensions obtained from recent simulations carried out by the present authors [22]. We first observe from Fig. 2 that, in contrast to the case of pure Ising domain growth, the scaled correlation functions show considerable curvature in the short-distance part at the early stage of ordering, and as the ordering proceeds further the scaled correlation function slowly approaches the pure Ising scaling function, gradually reducing its short-distance curvature. We may explain this slow approach to the asymptotic limit and the resulting scaling violation for any finite time span, in terms of the existence of a different length scale in our model in addition to the usual length scale of average domain size. Namely, we have point defects along the domain walls and the coarsening process involves not only the decay of the domain walls but also that of these point defects on the inversion walls. Hence the average separation between point defects offers another length scale to take into account in the ordering process, which can

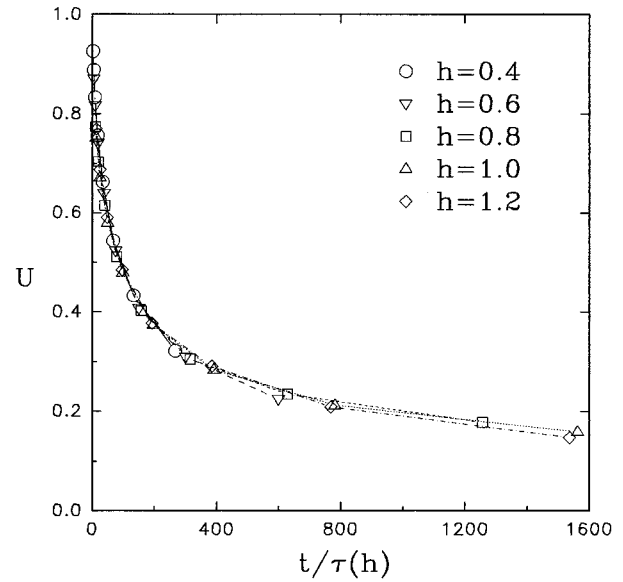


FIG. 4. Interpolation function  $U$  that represents the slow approach of the scaled correlation functions to the asymptotic limit. The functional form becomes universal, independent of the field  $h$ , when the time is rescaled with the same field-dependent time scale  $\tau(h)$  as used in Fig. 3(b).

break the self-similarity of the ordering process based on a single length scale.

In spite of this scaling violation based on the single dominant length scale, the length scale  $L_I(t)$  can still be considered as a meaningful length scale for the average size of the ordered domains, and one can extract the growth law exponents from data on  $L_I(t)$  for various values of the external fields  $h$ . These are shown in Fig. 3(a), from which we see that  $L_I(t)$  grows, at an early stage, with the power-law exponent of  $\phi_1 \approx 0.38$  and then it slowly crosses over into the

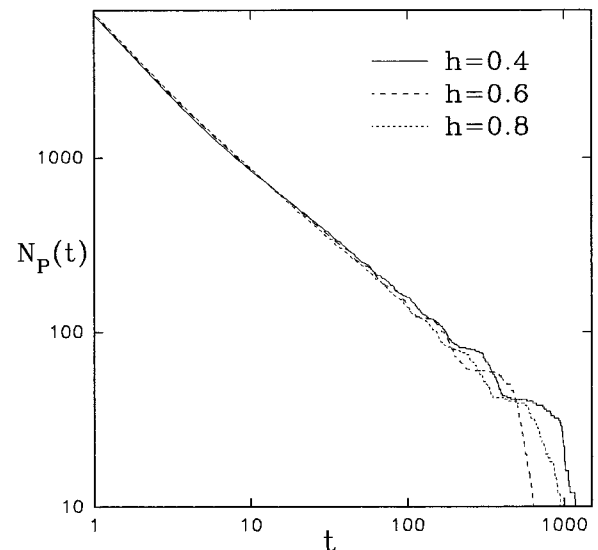


FIG. 5. Time dependence of the total number of point defects for a few values of the external magnetic field. It shows a power-law decay in time  $N_p(t) \sim t^{-\nu_p}$ , with  $\nu_p \approx 0.76$ .

late time exponent  $\phi_2 \approx 0.46$ , which is close to the pure curvature-driven growth exponent of  $1/2$ . As the magnitude of the magnetic field  $h$  increases, the time scale at which the crossover occurs tends to decrease, which is consistent with a dimensional analysis from Eq. (2), which gives  $\tau \sim 1/h^2$ .

From this observation, we may be tempted to try to collapse the time dependence of  $L_I(t)$  for various values of the external field  $h$ , by measuring the domain size  $L_I(t)$  in terms of the equilibrium wall width  $\xi \sim 1/h$  and the time  $t$  in units of  $\tau(h)$ , i.e.,  $hL_I(t) = G[t/\tau(h)]$ . We find that it is indeed possible to collapse  $L_I(t)$  for various values of  $h$ , which is shown in Fig. 3(b). For the best collapse the field dependence of the time scale  $\tau$  scales as  $\tau \sim 1/h^2$  for  $h < 1.0$ , consistent with the dimensional analysis, and  $\tau \sim 1/h$  for  $h \geq 1.0$ .

Collapse of  $L_I(t)$  for various values of the magnetic field  $h$  signifies that, even though the system does not possess self-similarity of the ordering process, there still exists a kind of regularity in the ordering process itself. This leads us to speculate that there may also exist a similar kind of regularity in the manner in which the rescaled correlation functions approach the asymptotic limit. We indeed find that the ap-

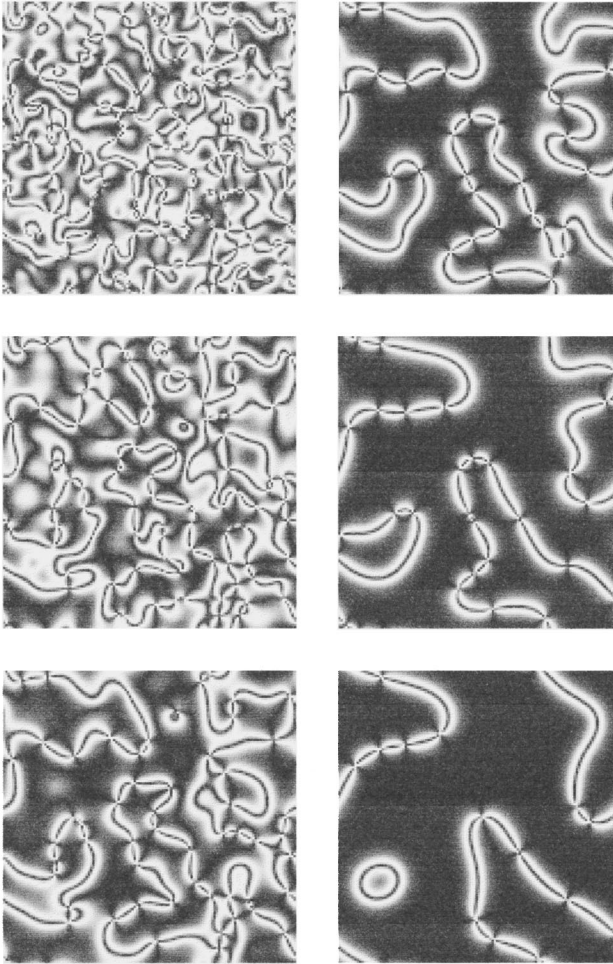


FIG. 6. Snapshots of the Schlieren texture at various times  $t=5, 10, 20$  (from top left down),  $40, 80, 160$  (from top right down) for  $h=0.4$  on a square lattice with linear size 128. We see the annihilation of point defects on the domain walls as the ordering proceeds.

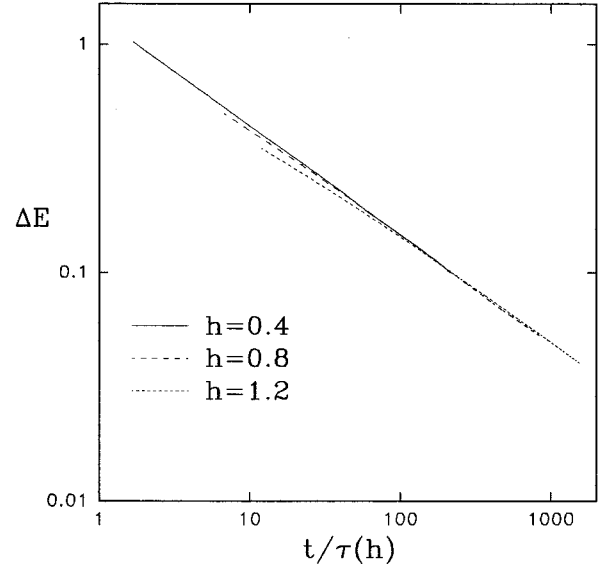


FIG. 7. Relaxation of the excess energy in the rescaled time  $t/\tau(h)$ . It exhibits a power-law form  $\Delta E \sim t^{-\nu_E}$ , with  $\nu_E \approx 0.48$ .

proach of the rescaled correlation functions  $F(x, t)$  to the asymptotic limit can be represented as

$$F(x, t) \equiv C[r/L_I(t), t] = f_I(x) + U(t/\tau(h))[f_0(x) - f_I(x)], \quad (13)$$

where  $f_I(x)$  is the Ising scaling function and  $f_0(x)$  the scaled correlation function at some reference initial time (here taken to be  $t=0$ ). The function  $U(t/\tau)$ , shown in Fig. 4, represents an interpolation function in time and evidently satisfies  $U(0)=1$  and  $U(\infty)=0$ . Note that the same time scale  $\tau(h)$  appears here as that used in the collapse of  $L_I(t)$ . When we tried a nonlinear fit of the form  $U(t/\tau) \sim 1/[1 + b(t/\tau)^\mu]$  with  $b$  a constant, we could get  $\mu \approx 0.6$ .

The time dependence of the average separation between point defects can be obtained from measuring the total number of point defects  $N_p(t)$ , which is shown in Fig. 5 for a few values of the external field. It exhibits a power-law decay in time  $N_p(t) \sim t^{-\nu_p}$  with  $\nu_p \approx 0.76$ , and this implies that the average separation between point defects goes as  $L_p(t) \sim 1/\sqrt{N_p(t)} \sim t^{0.38}$ , which coincides with the growth exponent of  $L_I(t)$  at the early time stage of the ordering process. Therefore, at this early time stage of ordering, the average domain size coincides with the average separation between point defects, and the short-distance behavior of the correlation function for the Ising-like order parameter is strongly influenced by the presence of point defects on the domain walls, resulting in the scaled correlation functions with larger curvature near the origin. At the late stage of ordering, the average domain size grows faster than the average separation between the point defects does, and therefore the effect of the point defects on the short-distance behavior of the correlation function becomes weaker, reducing the short-distance curvature of the scaled correlation functions.

Experimentally, the point defects are most clearly seen in the Schlieren texture in which the intensity of the light re-

flected from the liquid crystal sample placed between two polarizers with perpendicular polarization axes are measured. In numerical simulations, we can easily produce snapshots of such images, which are shown in Fig. 6, where the intensity is proportional to  $\sin^2(2\theta)$ ,  $\theta$  being the angle between a polarization axis and the director field. In this figure, a point defect can be identified as a point at which four bright (or dark) regions meet. We see that as mentioned above, the ordering process involves annihilations of point defects.

Another quantity of interest is the time dependence of the excess energy relaxation, shown in Fig. 7 for different values of the external field. Here, we can also rescale the data with time in units of  $\tau(h)$  and  $\Delta E$  in units of  $h^2$ . That is, we have  $\Delta E/h^2 = Y[t/\tau(h)]$ . We see that the excess energy relaxes in time as a power law of  $\Delta E \sim t^{-\nu_E}$  with  $\nu_E \approx 0.48$ , which is close to the behavior we can expect based on the characteristic features of Ising domain growth as mentioned earlier [see Eq. (12)].

#### IV. SUMMARY

We investigated numerically the coarsening and growth of Ising order associated with the field-induced domain walls

using the two-dimensional continuum time-dependent Ginzburg-Landau model based on a planar vector that includes a term breaking the  $O(2)$  symmetry, leaving Ising degeneracy of the ground states. We found a systematic scaling violation in the equal time correlation functions for the Ising-like order parameter, which may be attributed to the existence of a new length scale corresponding to the average separation between point defects residing on the domain walls. Some of the results obtained in the present simulations may be experimentally tested in smectic-*C* films under an external magnetic field.

#### ACKNOWLEDGMENTS

We thank Professor Noel Clark for a valuable discussion. This work has been supported in part by the KOSEF through Grant No. KOSEF-961-0202-009-1 and in part by the Basic Science Research Program, Ministry of Education, through Grant No. BSRI-95-2412 (B.K.), and by the KOSEF (J.R.L.).

- 
- [1] J. D. Gunton, M. San Miguel, and P. S. Sahni, in *Phase Transitions and Critical Phenomena*, edited by C. Domb and J. Lebowitz (Academic, New York, 1983), Vol. 8; H. Furukawa, *Adv. Phys.* **34**, 703 (1985); K. Binder, *Rep. Prog. Theor. Phys.* **50**, 783 (1987).
  - [2] A. J. Bray, *Adv. Phys.* **43**, 357 (1994).
  - [3] A. J. Bray, in *Phase Transitions and Relaxation in Systems with Competing Energy Scales*, edited by T. Riste and D. Sherrington (Kluwer Academic, Boston, 1993).
  - [4] G. F. Mazenko, *Phys. Rev. Lett.* **63**, 1605 (1989); *Phys. Rev. B* **42**, 4487 (1990); **43**, 5747 (1991).
  - [5] T. Ohta, D. Jasnow, and K. Kawasaki, *Phys. Rev. Lett.* **49**, 1223 (1982).
  - [6] K. Kawasaki, M. C. Yalabik, J. D. Gunton, *Phys. Rev. A* **17**, 455 (1978).
  - [7] A. J. Bray and S. Puri, *Phys. Rev. Lett.* **67**, 2670 (1991).
  - [8] F. Liu and G. F. Mazenko, *Phys. Rev. B* **45**, 0965 (1992).
  - [9] H. Toyoki, *Phys. Rev. B* **45**, 0965 (1992).
  - [10] G. F. Mazenko and M. Zannetti, *Phys. Rev. B* **32**, 4565 (1985).
  - [11] A. M. Somoza and R. C. Desai, *Phys. Rev. Lett.* **70**, 3279 (1993).
  - [12] P. G. de Gennes and J. Prost, *The Physics of Liquid Crystals*, 2nd ed. (Oxford, New York, 1994).
  - [13] A. P. Wong, P. Wiltzius, and B. Yurke, *Phys. Rev. Lett.* **68**, 3583 (1992); N. Mason, A. N. Pargellis, and B. Yurke, *ibid.* **70**, 190 (1993), and references therein.
  - [14] W. Helfrich, *Phys. Rev. Lett.* **21**, 1518 (1968).
  - [15] P. G. de Gennes, *J. Phys. (Paris)* **32**, 789 (1971).
  - [16] F. Brochard, *J. Phys. (Paris)* **33**, 607 (1971).
  - [17] For more details, see *Solitons in Liquid Crystals*, edited by L. Lam and J. Prost (Springer-Verlag, New York, 1992).
  - [18] R. Pindak, C. Y. Young, R. B. Meyer, and N. A. Clark, *Phys. Rev. Lett.* **45**, 1193 (1980).
  - [19] A. N. Pargellis, P. Finn, J. W. Goodby, P. Panizza, B. Yurke, and P. E. Cladis, *Phys. Rev. A* **46**, 7765 (1992).
  - [20] P. C. Hohenberg and B. I. Halperin, *Rev. Mod. Phys.* **49**, 435 (1979).
  - [21] G. Porod, in *Small Angle X-Ray Scattering*, edited by O. Glatter and L. Kratky (Academic, New York, 1983).
  - [22] J. -R. Lee, S. J. Lee, and B. Kim, *Phys. Rev. E* **52**, 1550 (1995).